JOURNAL OF GUIDANCE, CONTROL, AND DYNAMICS
Vol. 15, No. 3, May-June 1992

Control and Display Combinations for Blind Vertical Landings

J. A. Schroeder* and V. K. Merrick†
NASA Ames Research Center, Moffett Field, California 94035

Several hover control and display concepts were evaluated in flight on a variable-stability helicopter. The control and display concepts enable precise hover maneuvers, station keeping, and vertical shipboard landings in zero-visibility conditions and until now have been evaluated only in piloted simulations. A new display design method is presented that attempts to attain the same pilot-vehicle performance regardless of the level of control augmentation. The display design method was first examined analytically with the control dynamics in the context of the pilot's desired guidance strategy. Then, while fully hooded, three pilots performed landing-pad captures followed by vertical landings with attitude-rate-command/attitude-hold, attitude-command/attitude-hold, and translational-velocity-command control systems. Of the 28 piloted blind landings, 25 were within 5 ft and 14 were within 2 ft of the specified touchdown point.

Introduction

CURRENT AV-8B Harrier shipboard landings are restricted to weather minima of 300 ft ceiling and 1 mile visibility. To allow for the weather to degrade below these minima, adequate fuel is preplanned for landing at an alternate site. This visibility restriction and the need to carry contingency fuel limit the operational flexibility of the aircraft and warrant further research aimed at providing a blind landing capability for vertical/short takeoff and landing (V/STOL) aircraft.

Flight research into attaining this capability has been conducted previously via simulated-instrument-meteorological condition (IMC) approaches and landings in helicopters.[1-4] Most of these experiments examined automatic approaches and landings, but Ref. 1 also evaluated manual approaches and landings. In their summary, the authors of Ref. 1 stated that "although well-controlled approaches and landings could be performed manually with the flight director concept, pilot comments indicated the need for a better display which would more effectively integrate command and status information."[1]

A solution to the need for better displays has been the principal goal in recent control and display experiments aimed at enabling fixed-wing V/STOL pilots to perform all-weather approaches and vertical shipboard landings.[5-14] Until now, these concepts have been refined and evaluated only in fixed and moving-base piloted simulations. To stimulate further development of these concepts before flight tests using a modified YAV-8B Harrier,[14] a flight investigation was conducted on a variable-stability helicopter. The primary advantage of the helicopter is that it provides an efficient hovering platform for flight examination of the control and display concepts and pilot-vehicle operational issues. One of the disadvantages is that the helicopter has a comparatively high vibration environment that complicates the task of satisfactorily designing display element drive laws from noisy sensor signals. Another disadvantage is that the pilot's perception of the landing task could be influenced by the vibratory environment and peculiar ground effects associated with a twin rotor helicopter. However, it was judged that the tests would provide experience and design guidance before YAV-8B tests, with the added bonus of providing a useful contribution to the attainment of a helicopter manual blind landing capability.

This paper describes the flight equipment and discusses the control system and display design philosophy. Then, the flight task is described, followed by the pilot-display-vehicle performance results, including pilot ratings and opinions.

Equipment

The experiment was conducted in the CH-47B Variable Stability Helicopter,[15] wherein an evaluation pilot flies the fly-by-wire research system through conventional helicopter controls. Pilot inputs are sent to a digital flight-control computer (FCC) that in turn issues position commands to the full-authority-parallel cyclic and collective actuators. A safety pilot monitors the back-driven-control positions to allow disconnect of the research system to prevent hazardous operations.

A 4.9 in. square panel-mounted color display was used to depict the display symbology. The field of view subtended by the display was 8.8×8.8 deg. The time delay between a stick input and the movement of an element on the display owing to system hardware, such as filters and computational delays, was 90 ms. All visual cues were obtained from the panel mounted display only; outside visual cues were obscured completely with curtains and a pilot instrument hood.

The CH-47B was equipped with a comprehensive set of sensors and associated signal processing needed to implement the desired control and display systems. As depicted in the signal flow diagram of Fig. 1, variables subscripted with the letter c were used only by the control system, and variables subscripted with the letter d were used only by the display. Doubly subscripted variables were used by both the controls and the display. Aircraft horizontal positions were uplinked from a ground-based laser tracker. To generate the high-quality velocity and position data needed for precise landings, the raw accelerations, velocities, and positions were transformed to a common reference frame and processed in complementary navigation filters.[16]

Control and display configurations were tested before flight using the CH-47B onboard ground-simulation capabilities. During ground simulation, the display was as in flight. The aircraft's behavior was simulated with an eighth-order linear stability-derivative hover model. The model was driven by

Received June 20, 1990; revision received July 1, 1991; accepted for publication July 19, 1991.

*Aerospace Engineer, Flight Dynamics and Controls Branch. Member AIAA.

†Senior Research Engineer, Flight Dynamics and Controls Branch.

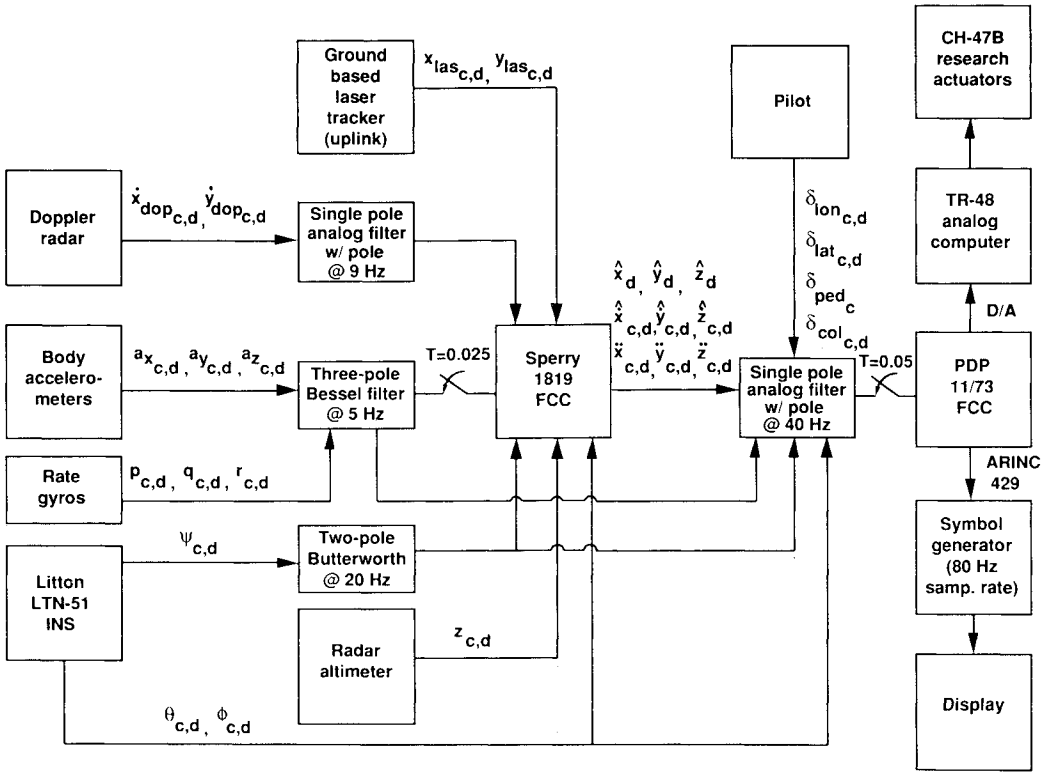

Fig. 1 CH-47B signal flow.

actuator commands generated from the same software as used in flight. The actuators, rotors, filters, and sensors were not modeled. Instead, a pure time delay of 200 ms which approximated all the unmodeled high-order dynamics, was incorporated into the simulation.

Control Law Description

Three longitudinal and lateral command/response control systems were tested: 1) attitude-rate-command/attitude-hold (RCAH), 2) attitude-command/attitude-hold (ACAH), and 3) translational-velocity command (TVC). Three height control systems were evaluated with the three longitudinal and lateral control systems: 1) YAV-8B (almost a vertical acceleration command system, 2) YAV-8B with added vertical damping, and 3) vertical-velocity command. The yaw control system was yaw-rate command without heading hold and remained invariant. The desired control-system dynamics and sensitivities for these control modes are listed in Table 1. These characteristics originated from NASA Ames simulation experience for full-authority controllers.[9]

The existing explicit-model-following flight-control system (MFCS) structure described in Ref. 17 was used to try to achieve the desired control/response characteristics for all axes except the TVC system. In this MFCS structure, a prefilter, representing the dynamics of the desired model to be followed, is placed after the pilot input. Here, the desired models are those of Table 1. The vector of errors between the model and aircraft states is sent through a proportional-plus-integral network for shaping and for eliminating steady-state model-following errors. To compensate for time delays, model accelerations are fed forward, and complementary filters are used in the heavily filtered attitude-rate-feedback paths to improve the bandwidth of the stabilization loops. It should be noted that the nature of the explicit-model-following structure results in faster vehicle disturbance rejection dynamics than the command response dynamics of Table 1. For example, the effective yaw damping to disturbances is higher than the value of $-2\ s^{-1}$ in the command model.

A different implementation was required for the TVC system. A modified application of the method developed in Ref. 5, with an example relevant to TVC in Ref. 8, was used here. The method is centered on an implicit-model-following scheme that incorporates state rate, or acceleration for a TVC system, as a feedback. Therefore, the structure is dubbed state-rate-feedback-implicit-model-following (SRFIMF). The outer loops and compensation described in Ref. 8 were wrapped around the inner attitude loops of the previous explicit-model-following system. A block diagram of the modified structure implemented on the CH-47B for the lateral axis is shown in Fig. 2. The effective inner-attitude loops of the controller are shown as the "model of aircraft with attitude

Table 1 Desired model dynamics

Axis	Command/ response type	Response	
Pitch (and roll)	Rate-command/ attitude-hold[a]	$\frac{\dot{\theta}}{\delta_{lon}} = \frac{\dot{\phi}}{\delta_{lat}} = \frac{8.73*3}{s+3}$	deg/s/in.
	Attitude-command/ attitude-hold[a]	$\frac{\theta}{\delta_{lon}} = \frac{\phi}{\delta_{lat}} = \frac{9.46*2^2}{(s+2)^2}$	deg/in.
	Translational-velocity command	$\frac{\dot{x}}{\delta_{lon}} = \frac{\dot{y}}{\delta_{lat}} = \frac{7.06*1.75^3}{(s+1.75)^3}$	ft/s/in.
Directional	Yaw-rate command[a]	$\frac{\dot{\psi}}{\delta_{ped}} = \frac{9.00*2}{s+2}$	deg/s/in.
Vertical	YAV-8B low vertical damping[a]	$\frac{\dot{h}}{\delta_{col}} = \frac{216.*0.02}{s+0.02}$	ft/s/in.
	YAV-8B high vertical damping[a]	$\frac{\dot{h}}{\delta_{col}} = \frac{6.90*0.62}{s+0.62}$	ft/s/in.
	Vertical velocity command[a]	$\frac{\dot{h}}{\delta_{col}} = \frac{8.36*0.88}{s+0.88}$	ft/s/in.

[a]Models for the Ref. 17 control system.

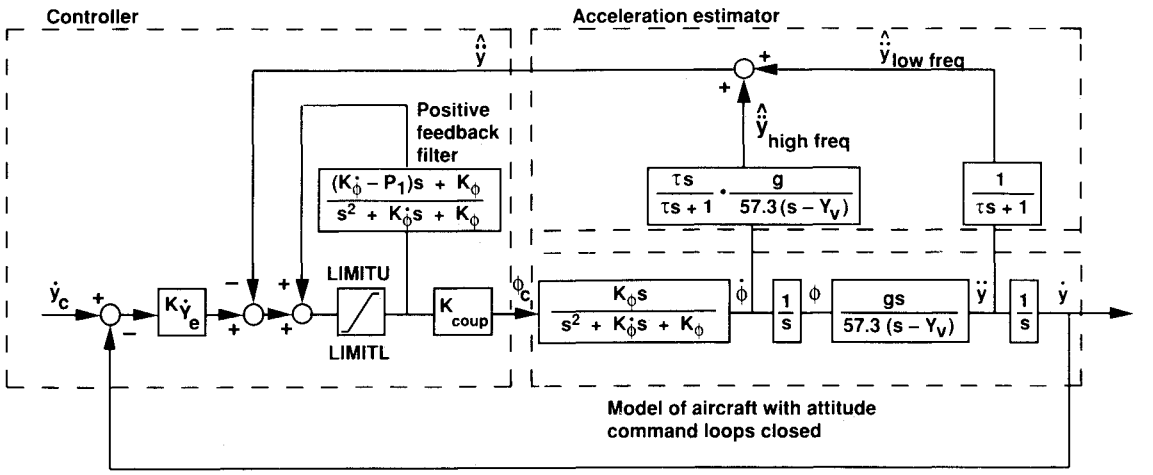

$K_{\dot{Y}_e}$ = 0.583 1/sec
$K_{\dot{\phi}}$ = 4 1/sec
K_{ϕ} = 4 1/sec^2
P_1 = 3 * ω_o = 3 * 1.75 = 5.25 1/sec
K_{coup} = 4.087 deg-sec/ft
Y_v = −0.137 1/sec
τ = 10 sec
LIMITU = 20/K_{coup} = 4.89 ft/sec^2
LIMITL = 20/K_{coup} = 4.89 ft/sec^2

Fig. 2 Translational velocity command controller.

command loops closed." For SRFIMF compensation, the positive feedback loop containing the limiter cancels the poles of the inner attitude loops, places a pole at the origin for self-trimming, and inserts a pole on the real axis to make the filter realizable. The remaining gains are determined using pole placement to achieve three real-axis poles at −1.75 rad/s.[8] Two modifications from the originally developed control law are that 1) the inner attitude loops were closed by an explicit-model-following structure rather than by an SRFIMF attitude system structure, which requires angular accelerometers, and 2) a complemented value of linear acceleration from both accelerometer and angular-rate measurements was used (Fig. 2). The latter was required because of the severe vibratory CH-47B environment.

Control System Response Identification

Since any system will have model following errors, it is important to quantify these errors. Using frequency domain identification techniques,[18] the dynamics of all three command/response types were identified during flight using pilot-generated frequency sweeps in the roll axis. Table 2 shows the results in several forms. The low-order equivalent fits were obtained by using NAVFIT[19] on the resulting identified frequency responses. Available flight-test time precluded the identification of the control dynamics in the other axes.

The definitions of bandwidth and phase delay used in Table 2 are given in Ref. 20. The identified RCAH system falls within the level 2 boundaries for both ADS-33[20] and the proposed revisions to MIL-F-83300.[21] The flight system time delay causes this degradation from level 1 per the bandwidth definition. The ACAH system falls within the level 1 boundaries for Ref. 20 and the level 2 boundaries for Ref. 21. The effective first-order time constant of the TVC system is 0.5 faster than the 2.5 s minimum specified time of Ref. 20, but it is within the recommended boundaries of Ref. 22 and was classified as "desired" in Ref. 23. Other specification compliance testing, such as disturbance rejection criteria, was not conducted.

From the identifications, only the RCAH system consistently falls within level 2 boundaries, whereas the ACAH and TVC systems should have been satisfactory to perform the task discussed later. Pilot comments stated that "the horizontal control command/response sensitivities and dynamics were well balanced and predictable" for each system. It should be noted that, although each individual axis was satisfactory, their combined use in a challenging multiaxis task (such as the one described later) may not produce commensurate handling quality ratings.[24]

Display Laws

Each element of the hover display is identified in Fig. 3. A complete description of the display with the drive laws for each element, except for the new acceleration cue law described herein, is given in Ref. 25. The display integrates both horizontal and vertical situation information. The horizontal view is from above the aircraft, and the vertical view is from

Table 2 Identified roll axis control dynamics

Command/ response type	Dynamics	Roll attitude bandwidth, rad/s	Phase delay, ms	Equiv. first-order τ, s
Rate-command/ attitude-hold, deg/s/in.	$\frac{\dot{\phi}}{\delta_{lat}} = \frac{8.73*2.78}{s+2.78} e^{-0.145s}$	1.60	157	—
Attitude-command/ attitude-hold, deg/in.	$\frac{\dot{\phi}}{\delta_{lat}} = \frac{9.46*0.862*4.80}{(s+0.862)(s+4.80)} e^{-0.196s}$	2.73	175	—
Translational-velocity command, ft/s/in.	$\frac{\dot{y}}{\delta_{lat}} = \frac{7.06*2.10*1.30^2}{(s+2.10)[s^2+2(0.646)(1.30)s+(1.30)^2]} e^{-0.175s}$	4.02	—	2.0

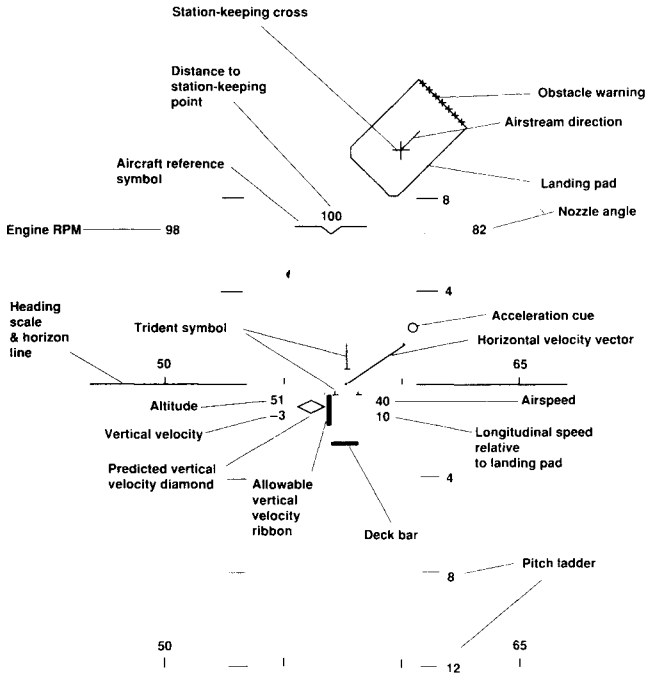

Fig. 3 General arrangement of hover display.

behind the aircraft. The three-legged trident symbol, fixed in the center of the symbology, represents the landing gear and the noseboom of the YAV-8B to scale relative to the rectangular landing pad. This pad represents the 40 × 70 ft pad on the *Spruance*-Class DD-963-type destroyer. If the trident remains within the horizontal landing-pad geometry during the descent to landing, the aircraft will remain clear of obstacles, and all gear will touch within the deck perimeter. A horizontal velocity vector and an acceleration cue originate at the trident center. In the steady state, the tip of the velocity vector will coincide with the center of the cue. The presentation format of the horizontal groundspeed vector dates from 1967[26] and has been studied in several formats by Dukes et al.[27] The addition of the acceleration cue to the velocity vector originated in 1974,[28] and a version of this combination is used in the AH-64 Apache.[29]

Vertical position above the touchdown point is represented in analog form by the distance between the deck bar and the two bottom trident gear symbols. The vertical velocity information is presented by both a digital readout of current sink rate (in ft/s) relative to the landing pad and a vertical velocity diamond. The diamond's position is a combination of the current vertical velocity and washed-out throttle position. Thus, it represents a prediction of vertical velocity and can be used in a manner similar to the acceleration cue to assist the pilot in anticipating the effects of control inputs. An allowable vertical-velocity ribbon is shown off the left trident gear. The length of this ribbon is dependent on the aircraft's vertical velocity, the ship deck's vertical velocity, and the aircraft landing gear's vertical velocity structural limit.[25] The pilot's descent task is to keep the predicted vertical-velocity diamond within this allowable vertical-velocity ribbon to prevent gear structural damage upon shipboard landing. With a moving ship deck, even in a stabilized hover, the allowable vertical-velocity ribbon changes in length owing to the vertical velocity of the ship deck. For these land-based tests, its length remained fixed at the allowable vertical velocity of -9 ft/s. The remaining display elements are status variables and are self-explanatory.

To maximize the display's usefulness, it needs to be examined in the context of the goals that the pilot is trying to achieve in performing the task. In broad terms, this task is to control the vehicle's position accurately. More specifically, the task involves both maintaining a stable position over the landing pad (regulating errors) as well as quickly maneuvering the aircraft to a stable hover over the pad from any moderately large offset. Accordingly, a simple, reliable, and effective control strategy for the pilot is desired that will result in his achieving or maintaining the desired position. To ease the mental workload, the conveyance of this strategy should preferably involve the use of a single display element for each control axis or each pilot control inceptor.

First, consider the task of maintaining position over the pad. Suppose the pilot, by some means, was able to keep the tip of the velocity vector in the center of the pad during acquisition. At the steady state when the vector attains zero length, the required performance is achieved. Dynamically, when the position error is nonzero and the velocity tip is still fixed at the pad center, a stable exponential convergence is achieved with a time constant determined by the displayed position and velocity scalings. Here, the pilot effectively used the display as an analog computer to solve the differential equation

$$K_{\dot{x}}\dot{x} + K_x x = K_x x_c, \qquad x(0) = x_0 \tag{1}$$

where x_0 is some initial condition and x_c and x are the commanded and actual positions of the aircraft. The display scaling variables $K_{\dot{x}}$ and K_x convert the aircraft's relative velocities and positions with respect to the pad into display degrees. They have the units deg/ft/s and deg/ft, respectively.

This simple control strategy involves using pure situational display information to achieve a guidance objective. Unfortunately, keeping the velocity vector in the center of the pad is typically a difficult piloting task without additional displayed lead information. Most production hovering vehicles have several integrations between the cockpit controls and the vehicle's velocity response. These integrations significantly reduce the open-loop phase and gain margins (relative to the pilot), often resulting in severe stability and control problems.

The addition of another display element, the acceleration cue, provides a way by which the stability and control problems associated with a typically sluggish velocity response may be overcome. First, by referencing the cue to the tip of the velocity vector, the design can ensure that the cue will lead the velocity vector around the display in response to control inputs and thereby enhance overall stability. Second, since the steady-state length of the velocity vector is controlled by the position of the cue, then 1) if the pilot maintains the cue on the desired position (i.e., the center of the pad), and 2) if the pilot-vehicle-display system is stable, the aircraft position and the desired position will eventually coincide.

For illustrative purposes, a sequence of events in a one-dimensional closure using the acceleration cue is shown in Fig. 4. Figure 4a shows that the pilot is moving the aircraft to the pad, which is shown at a distance x_c from the aircraft ($K_x x_c$ in display deg), and has moved the controls to establish a velocity by placing the acceleration cue in the center of the pad. The cue position relative to the trident is A_x. In Fig. 4b, the aircraft has moved a distance x ($K_x x$ in display deg), and the pilot has provided the necessary compensation to maintain the cue in the center of the pad. In Fig. 4c, the aircraft is hovering over the desired position. The pilot sees the pad symbol move on the display rather than the aircraft fixed trident. Note that the pilot provides the necessary compensation to position the cue at the center of the pad always. This piloting strategy is shown as a feedback control system with a command of x_c in Fig. 5. The pilot, represented here for simplicity by a gain K_p, acts on the error between the pad and the cue position as shown. When the inner display loop is closed around the pilot gain in Fig. 5, the result is

$$\frac{\delta_{\text{lon}}}{\delta_{\text{pad}}}(s) = \frac{K_p}{1 + K_p(A_x(s)/\delta_{\text{lon}})(s)]} \tag{2}$$

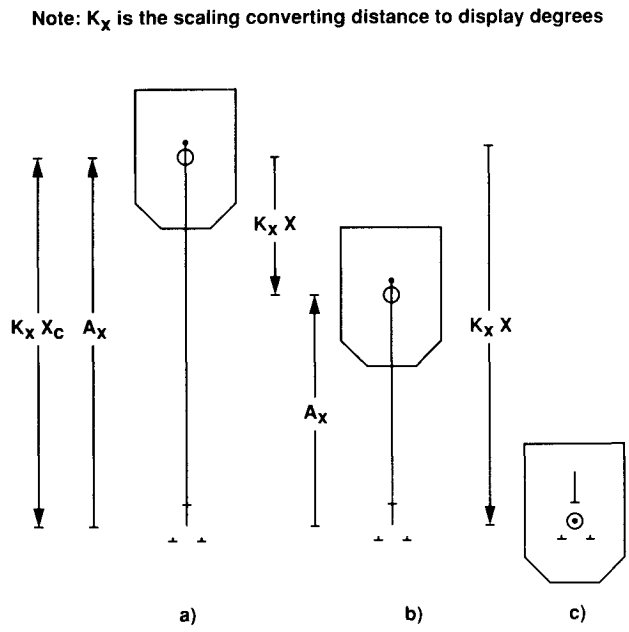

Fig. 4 Sequence of display closure to desired position.

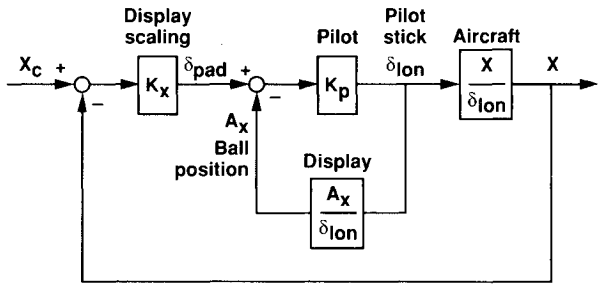

Fig. 5 Block diagram of the pilot-vehicle-display dynamics.

As the pilot gain becomes very large, which implies that the cue is always on the pad, the inner cue position loop may be approximated as $\delta_{lon}(s)/A_x(s)$, which is the inverse of the display transfer function $A_x(s)/\delta_{lon}(s)$. The inverse of the display dynamics when combined with the vehicle command/response dynamics $x(s)/\delta_{lon}(s)$ results in the open-loop transfer function $K_x x(s)/A_x(s)$, from which the total system performance can be readily analyzed. Typically for compensatory displays, the controlled-element dynamics, $A_x(s)/\delta_{lon}(s)$, are designed to achieve integrator-like (K/s) characteristics in the region of pilot-vehicle-display crossover.[30,31] However, since 1) this display is a pursuit rather than a purely compensatory display, and 2) the attendant delays in the inner loop can degrade the resulting position outer loop phase margin, a different approach was used here.

Instead, a desired type of closure velocity dynamics was used to develop the structure of the controlled-element dynamics. That is, if the pilot uses the acceleration cue to command a desired velocity, then the closure of the velocity vector to the cue, or the aircraft velocity to the commanded velocity, will have desirable characteristics.

As an example of this procedure, an ACAH system may be represented by

$$\frac{\theta}{\theta_c}(s) = \frac{K_\theta}{s^2 + K_{\dot\theta} s + K_\theta} \tag{3}$$

where θ_c is proportional to δ_{lon}. Then, since for small perturbation angles about trim $\dot{x}(s) \approx [-g/(s - X_u)]\theta(s)$, the vehicle

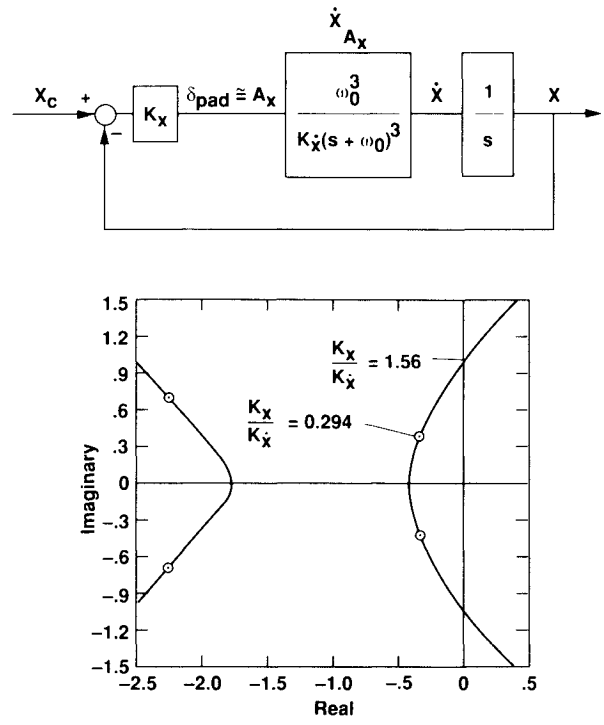

Fig. 6 Position loop closure assuming large pilot gain.

velocity response in hover is

$$\frac{\dot x}{\theta_c}(s) = \frac{-gK_\theta}{(s - X_u)(s^2 + K_{\dot\theta} s + K_\theta)} \tag{4}$$

where X_u is the aircraft longitudinal-velocity damping. It has been shown previously that three coincident real-axis roots between aircraft velocity and stick position are one way to achieve desirable dynamics for TVC systems.[23] Although the level of vehicle control augmentation may be reduced, the display may be designed to provide the pilot with the compensation required to still achieve velocity dynamics with three coincident real roots relative to a commanded velocity (acceleration cue position) on the display. With that design goal, the vehicle and display dynamics may be combined to achieve

$$\frac{\dot x}{A_x}(s) = \frac{\dot x}{\theta_c}(s)\frac{\theta_c}{A_x}(s) = \frac{\omega_o^3}{K_{\dot x}(s + \omega_o)^3} \tag{5}$$

where $K_{\dot x}$ converts the commanded velocity to A_x in display deg. Figure 6 shows a block diagram of the structure including the selected form of $\dot{x}(s)/A_x(s)$. Combining Eqs. (4) and (5) gives the relationship between the commanded pitch angle and the acceleration cue needed to attain the desired velocity response:

$$\frac{\theta_c}{A_x}(s) = \frac{\omega_o^3(s - X_u)(s^2 + K_{\dot\theta} s + K_\theta)}{-gK_\theta K_{\dot x}(s + \omega_o)^3} \tag{6}$$

Inverting and changing the commanded pitch attitude to stick position with $\theta_c(s) = (\pi/180)K_{sens_\theta}\delta_{lon}(s)$, where K_{sens_θ} is the pitch command sensitivity in deg/in.

$$\frac{A_x}{\delta_{lon}}(s) = \frac{-gK_\theta K_{\dot x} K_{sens_\theta}(\pi/180)(s + \omega_o)^3}{\omega_o^3(s - X_u)(s^2 + K_{\dot\theta} s + K_\theta)} \tag{7}$$

Equation 7 provides an explicit relationship between the acceleration cue position $A_x(s)$ and the stick position $\delta_{lon}(s)$. Equation (4), with an added integration and scaling change, can be cast in the form x/δ_{lon}, and this equation, along with Eq. (7), provides the transfer functions in Fig. 5.

The total dynamic behavior of the pilot, display, and vehicle may be determined by closing the position loop in Fig. 6. The position-to-velocity scaling ratio ($K_x/K_{\dot{x}}$) is the important factor governing the position response dynamics of the system. This ratio is directly proportional to the root-locus gain for the loop and is used to provide an acceptable compromise between speed of response and stability. The resulting position dynamics shown by the root locus of Fig. 6 may be well damped, poorly damped, or unstable even though the velocity response to a fixed-cue position is stable with no overshoot. For the flight experiment, the $K_x/K_{\dot{x}}$ ratio was 0.294 s^{-1}. Since a free integrator exists in the open loop, and since for the gain chosen the resulting system is stable, the system will have zero steady-state error to step inputs. If this ratio increases to 1.56 s^{-1} by making the display more sensitive to position errors or less sensitive to velocity errors, the closed loop will become unstable (Fig. 6).

Note that when using the cue to establish a given velocity, the open-loop dynamics given by Eq. (5) are without an extra integration in the denominator, and a position loop is not closed. Thus the velocity response to a fixed-cue position relative to the trident symbol has three coincident real roots.

In lieu of using Eq. (7) to generate the acceleration cue signal A_x, an alternative mechanization using $\dot{x}$, $\ddot{x}$, and θ_c signals from the aircraft sensors was used. From Eq. (5)

$$A_x(s) = K_{\dot{x}}\dot{x}_c(s) = \frac{K_{\dot{x}}(s+\omega_o)^3}{\omega_o^3}\dot{x}(s) \tag{8}$$

which may be rewritten in the form

$$A_x(s) = K_{\dot{x}}\dot{x}(s) + \frac{3K_{\dot{x}}}{\omega_o}\ddot{x}(s) + K_{\dot{x}}\frac{s(s+3\omega_o)}{\omega_o^3}\dddot{x}(s) \tag{9}$$

Substituting the approximate expression for longitudinal acceleration in terms of pitch attitude in Eq. (9)

$$A_x(s) = K_{\dot{x}}\dot{x}(s) + \frac{3K_{\dot{x}}}{\omega_o}\ddot{x}(s) - K_{\dot{x}}\frac{s^2(s+3\omega_o)g}{\omega_o^3(s-X_u)}\theta(s) \tag{10}$$

For an ACAH system, combining Eqs. (3) and (10) gives

$$A_x(s) = K_{\dot{x}}\dot{x}(s) + \frac{3K_{\dot{x}}}{\omega_o}\ddot{x}(s) - K_{\dot{x}}K_\theta\frac{s^2(s+3\omega_o)g}{\omega_o^3(s-X_u)(s^2+K_{\dot{\theta}}s+K_\theta)}\theta_c(s) \tag{11}$$

Equations (7) and (11) are equivalent. From Eq. (11), the acceleration cue position is shown to be biased from the velocity vector [$K_{\dot{x}}\dot{x}(s)$] by an acceleration term and a term consisting of a third-order washout filter on the commanded pitch attitude. The values used in Eq. (11) are listed in Table 3.

The form of the RCAH cue law is changed by a modification in the stick washout filter by substituting Eq. (3) in the previous development with

$$\frac{\theta}{\theta_c}(s) = \frac{K_{\theta_R}}{s(s+K_{\theta_R})} \tag{12}$$

For large pilot gain, this RCAH cue law results in the same total velocity dynamics. The form of the TVC acceleration-cue law is simply $A_x = K_{\dot{x}}\dot{x}_c$, where $\dot{x}_c = K_{\text{sens}_{\dot{x}}}\delta_{\text{lon}}$. The constant $K_{\text{sens}_{\dot{x}}}$ is the TVC system sensitivity. Here, the control system achieves the desired velocity dynamics, and the pilot may place the cue at the desired location on the display with a constant stick position. Thus, for large pilot gain, the previous display design procedure ensures that the aircraft will have a similar response to the acceleration-cue-position pilot-loop closure for all three control systems.

The frequency response of $A_x(s)/\delta_{\text{lon}}(s)$ is shown in Fig. 7 for the TVC, ACAH, and RCAH systems. The magnitude characteristics for the ACAH system are K/s-like at low frequencies, and they blend to a K-like response at high frequencies. Previous display work has shown this combination to be perhaps better than having K/s characteristics at all frequencies by relieving the pilot of the need to provide high-frequency lead to compensate for possible poor phase margins in the pilot-vehicle-display loop.[31] Experience at NASA-Ames has also shown that, for the landing task with pursuit displays, pilots tend to prefer immediate controlled-element response to stick inputs, which again indicates the preference of a high-frequency K-like response.[32] In fact, a recent investigation illustrated that for different hovering tasks with pursuit displays, pilots preferred the high frequency K-like display laws over the K/s-like display laws.[33]

The RCAH cue law in Fig. 7, with $\delta_{\text{lon}}(s) = K_{\text{sens}_{\dot{\theta}}}\dot{\theta}_c(s)$, is K/s^2 followed by a blend to K at high frequencies. The TVC cue law is simply a gain at all frequencies. Thus, this design technique results in cue-to-stick dynamics that are different as a function of aircraft dynamics. This result is unlike design procedures that equalize the display dynamics to make the cue-to-stick dynamics invariant between different sets of control dynamics; this latter method results in different aircraft responses among different control configurations for the same guidance task.

It is interesting to contrast the previous display design technique and philosophy with other techniques. For example, Ref. 34 focuses primarily on changes in the predictive nature of the cue to satisfy pilot-centered workload goals. In that work, the resulting vehicle performance was discussed for the cue always at the pad center and driven with acceleration. When additional lead was introduced into the cue, the result-

Table 3 Display variable values

Variable	Value
$K_{\dot{x}}$	0.202 deg/ft/s
K_x	0.0594 deg/ft
ω_o	1.75 rad/s
K_θ	4.00 $1/s^2$
$K_{\dot{\theta}}$	4.00 1/s
K_{θ_R}	3.00 1/s
X_u	−0.0210 1/s
g	32.2 ft/s^2
K_{sens_θ}	9.46 deg/in.
$K_{\text{sens}_{\dot{\theta}}}$	8.73 deg/s/in.
$K_{\text{sens}_{\dot{x}}}$	7.06 ft/s/in.

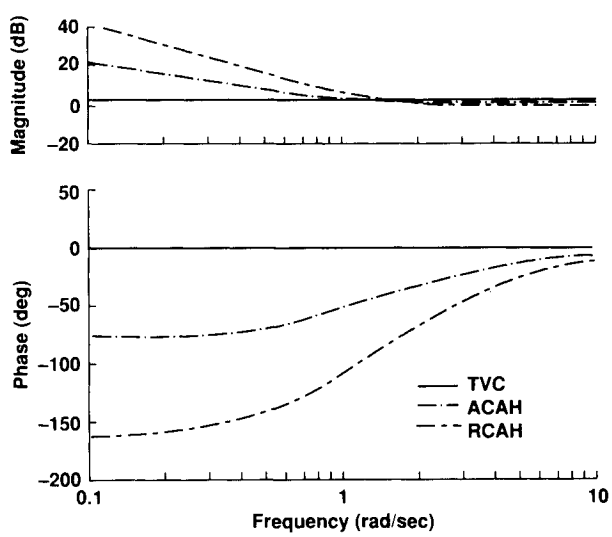

Fig. 7 $A_x(s)/\delta_{\text{lon}}(s)$ for velocity, attitude, and rate command display laws.

ing performance implications were evaluated empirically in piloted simulation instead of as a part of the design technique.

On the other hand, the design approach taken here is to achieve acceptable closed-loop performance with each cue design. The subsequent pilot-centered workload implications are now evaluated empirically. In certain instances, therefore, this procedure may sacrifice the pilot-centered workload goals. But the converse can also be troublesome: satisfying the classical pilot-centered compensation requirements in the inner loop may sacrifice acceptable closed-loop performance in the outer loop. The tradeoff between closed-loop performance and pilot-centered workload goals is especially crucial as the level of vehicle control augmentation is reduced. This tradeoff has not yet been fully quantified and is the subject of future work.

The performance and workload tradeoff when more lead is introduced into the display design has been discussed previously in Ref. 35. However, for disturbance-free environs, the applicability of this tradeoff is apparent only when the display is in the feedback path. This situation exists for the hover display design in this paper because the acceleration cue is not driven by the pad error. Thus, the zeros introduced in that path to achieve K/s or K-like behavior of the acceleration cue are not zeros of the closed-loop system. They are, in fact, approximately where the closed-loop poles will be. As more low-frequency lead is introduced into the cue, the closed-loop system slows down, causing performance to degrade. On the other hand, when displays are used in purely compensatory tasks, such as following localizer or glideslope bars (where the error can be designed as the input to the display), the display dynamics are in the forward path. For this case, the zeros introducing the lead are also the closed-loop zeros. Now, up to a certain point, the display may be designed to achieve low workload and good performance simultaneously. Yet, for flight applications with poorly augmented vehicles, it is difficult to achieve satisfactory flying qualities with the display rather than with the flight controls, since with the display the pilot has to supply continuous control and attention to reject disturbances.

Flight Task Description

The task originated 43 ft aft and 43 ft to the left or right of the designated touchdown point. The initial landing gear altitude was 43 ft (50 ft c.g. altitude), although pilots sometimes inadvertently started at 50 ft. From a stabilized hover at the initial point, pilots were instructed to perform a horizontal capture at constant altitude and heading to a point vertically above the designated touchdown point. Desired performance in altitude and heading for the horizontal capture was ± 5 ft and ± 2 deg, respectively. Adequate performance was ± 10 ft and ± 5 deg, respectively. After stabilizing, a vertical landing was performed. A desired landing performance of within 2 ft of the designated touchdown point was chosen for use with the Cooper-Harper handling qualities rating scale[36] because current visual AV-8B large deck operations (amphibious assault ships) desire lateral errors from the ship centerline to be less than 2 ft. With each control and display combination, the pilot maneuvered the aircraft using the display for initial familiarization. Then, he performed a minimum of three landing profiles before giving a handling qualities rating and comments in response to a questionnaire.

Table 4 Surface wind conditions

Day	Runway and aircraft desired heading, deg	Wind direction mean, deg	Wind magnitude mean, kt
1	300	333	9.5
2	300	349	8.7
3	300	327	9.1
4	300	342	11.3

Day	Wind magnitude std. dev., kt	Wind magnitude range, kt
1	2.0	3.8–30.1
2	1.8	4.3–15.5
3	1.7	4.5–16.7
4	2.0	5.1–18.0

Results and Discussion

Task Performance

The 28 simulated-IMC landings shown later were conducted on four different days with surface wind conditions shown in Table 4. As shown, the tests were conducted with a right-quartering headwind of approximately 10 kt with gusts up to as high as 30 kt.

Figures 8 and 9 show typical in-flight X-Y and Z-Y aircraft position crossplots for the task using the TRC, ACAH, and

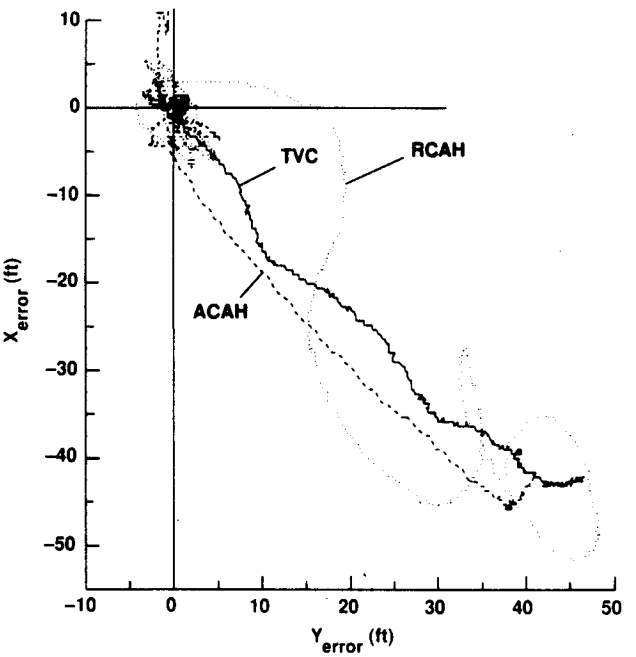

Fig. 8 X-Y vehicle position for pad capture task.

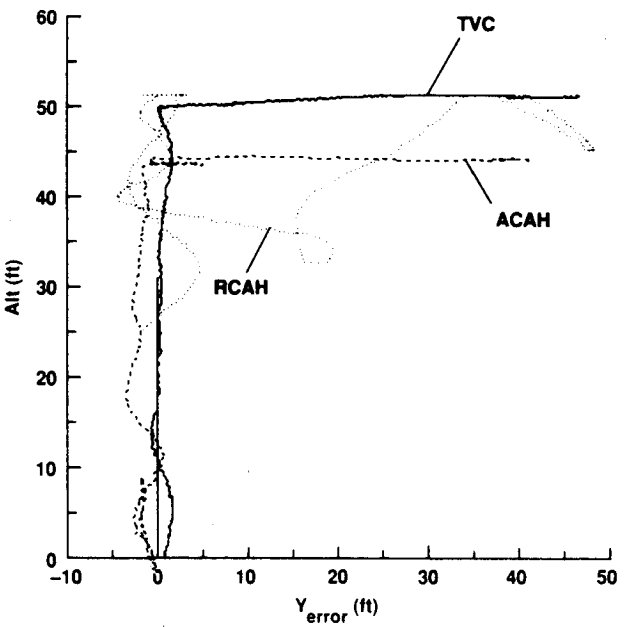

Fig. 9 Z-Y vehicle position for pad capture task.

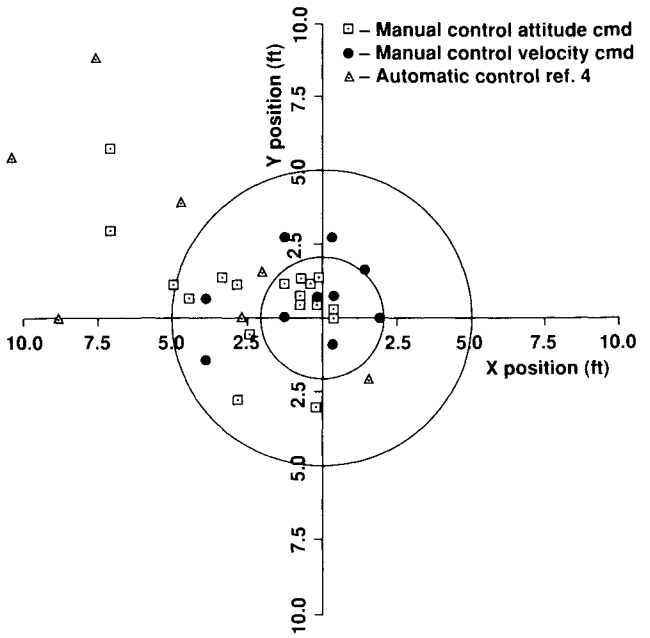

Fig. 10 Landing performance.

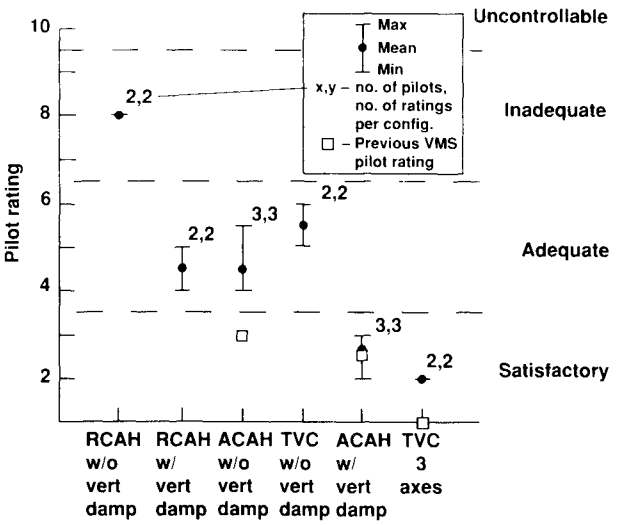

Fig. 11 Pilot ratings for ground simulation.

RCAH systems. In these figures, both the ACAH and RCAH systems had added vertical damping, whereas the TVC system had vertical velocity command. As shown, tracking performance was degraded between the TVC and the ACAH systems. A further marked degradation occurs between the ACAH and RCAH systems, which may be due to the display design philosophy as discussed later. With the RCAH system, all three pilots did not feel comfortable landing the aircraft under the hood, and as a result, the task was terminated before landing. Station-keeping excursions became larger nearer the ground, owing to the randomly increasing downwash distrubances. The task took 20 s longer to perform with the TVC system than with the ACAH system, with almost all the extra time allotted to a less aggressive horizontal capture.

All three pilots exhibited a tendency to lessen their aggressiveness with the TVC system in flight. Pilot comments suggest that the principal cause of this reduced aggressiveness is related to the aircraft attitude being controlled indirectly, that is, by the difference between the commanded velocity (stick position) and actual velocity (Fig. 2). A sudden stick input produces a transient overdrive of the attitude before reaching a value consistent with the commanded velocity. Currently, pilots obtain their hovering experience in helicopters and V/STOL aircraft that exhibit a one-to-one correspondence between stick position and either attitude or attitude rate and feel uncomfortable with the unusual dynamic relationship between stick position and vehicle attitude caused by the TVC system. A reasonable conjecture is that they seek to minimize the strange sensation by lessening the aggressiveness of their stick inputs and in particular avoiding sudden large stick inputs. An additional contributing factor may be that the same stick gradient was used for all three control systems. This effect resulted in a higher stick force required to establish a given velocity with the TVC system than with the direct attitude control systems.

Touchdown performance for the TVC and ACAH systems with vertical damping is shown in Fig. 10. The two circles centered at the designated touchdown point represent the desired and adequate performance touchdown levels for the task. Roughly 50% of the landings with each system were within the desired 2 ft radius standard. Although three points lie outside the adequate performance standard for the ACAH system, whereas all landings with the TVC system were at least adequate, it is still difficult to judge from Fig. 10 which system is superior. It should be noted that the ACAH system was used for initial system development, and so approximately twice as much time was spent training with this system than with the other two systems.

Comparing these results with those from other experiments, Ref. 1 documents the only other nonautomatic simulated-IMC landing performance, which was approximately 10 ft from the desired touchdown point. Automatic control touchdown accuracies from Ref. 4 are shown in Fig. 10 for comparison. Whereas a general improvement in accuracy is shown for the manual landings compared with the Ref. 4 automatic landings, this performance increase is also accompanied by a pilot workload penalty as discussed in the next section.

Pilot Ratings and Comments

Simulation

Figure 11 shows previously unpublished simulation data for a modified YAV-8B Harrier aircraft using the NASA Ames Vertical Motion Simulator (VMS) along with results from the CH-47B onboard ground-simulation evaluations. The RCAH system flown in this flight experiment was not simulated during full IMC in the VMS and is not shown on Fig. 11. During VMS evaluations, the TVC system received a pilot rating of one.

It is clear from the CH-47B simulation results in Fig. 11 that improved vertical axis dynamics improve pilot ratings considerably. The improvement was much greater for the TVC system than for the ACAH system (change of 3.5 against 2 pilot ratings). With the TVC system, vertical velocity command is present (here the pilot had an electrical deadband to find a zero command) rather than just vertical damping as with the ACAH system. Figure 11 shows that without vertical damping, the pilots were less at ease with the TVC system because the need to concentrate on the vertical task made it hard to adapt to the different and unaccustomed technique needed with this system. In fact, without the vertical damping, the pilots stated that the workload required to control the vertical axis was greater than that required to control the horizontal axes. The addition of vertical damping reverses the division of work by dramatically reducing the concentration needed for the vertical task. The workload reduction gives the pilot the opportunity to act with more deliberation and to concentrate on refining a flying technique that capitalizes on the velocity stability and self-trimming inherent in the TVC system.

Flight Test

Figure 12 shows the in-flight pilot ratings during simulated IMC. It is immediately apparent that the flight ratings are not as favorable as the simulation ratings. Whereas in simulation

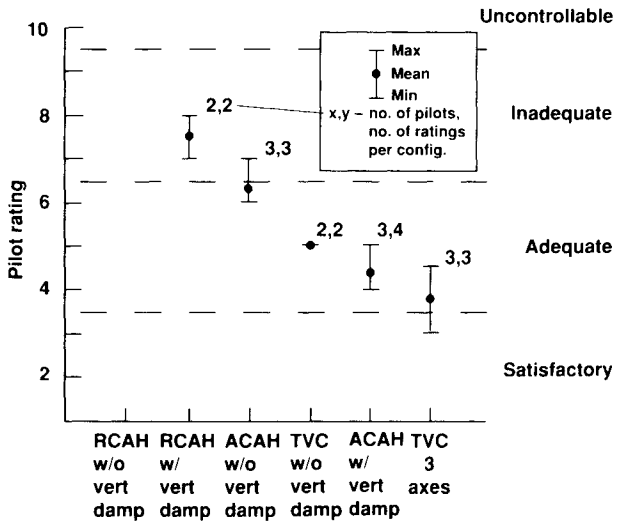

Fig. 12 Pilot ratings for flight: simulated IMC.

both the TVC and the ACAH systems were solid level 1 (satisfactory), during flight both of the average ratings moved into the level 2 (adequate) region, with the best rating for the TVC system in the level 1 region. All pilots felt the simulation was "tighter" than flight. Factors contributing to this degradation include 1) noisome rotor vibration in flight, 2) imperfect sensing in flight, 3) external disturbances in the form of winds, turbulence, and downwash effects near the ground during flight, and 4) degraded model following in fight. However, pilot opinion suggested that the model-following degradations were minor, since all pilots felt that the command/response characteristics of all three control systems were satisfactory during flight.

Also apparent is that the effect of adding vertical damping to the TVC and ACAH systems differed from the simulation. Now the improvement in pilot rating was less for the TVC system than for the ACAH system (1 against 2). The ability of the pilot to close a sensory vertical feedback loop in flight made the task less difficult than in the CH-47B ground simulation. Also, only the ratings for the TVC system had a spread reaching into the level 1 region during flight.

The pilots were all in agreement about the need for vertical damping. One pilot stated "without vertical damping, the presence of an unguarded vertical axis integrator (no steady-state velocity) disallows inattentiveness on the part of the pilot who, without any proprioceptive throttle-control position cue, can only monitor the display continually to be assured that unsafe altitudes and rates of descent are not accumulating." Another pilot stated that "without heave damping any additional intrusion, such as to check engine instruments or to respond to a radio call, would have required aborting or suspending the task."

Landings were also performed with the RCAH system in visual conditions with and without vertical damping. To perform this task, the pilot used the display to provide the guidance for landing precision and outside visual cues to supply the information needed to provide equalization to stabilize the aircraft's attitude. The workload for the task performed in this manner was very much reduced relative to that when the task was performed hooded. The aircraft could be flown down to touchdown with pilot ratings of 3–4 for the vertically damped case. These tests clearly indicated that, with an aircraft control system needing substantial pilot equalization, the cues offered by the tested display did not substitute for those of the visual scene. The major display deficiency, in this respect, is that it did not provide a sufficiently compelling awareness of changes of aircraft attitude and attitude rates. Another indication of this deficiency is that heading control required conscious attention in simulated IMC but not in visual conditions. The RCAH acceleration cue law also had low frequency K/s^2 characteristics (Fig. 7) that added to pilot workload by requiring the pilot to supply low-frequency lead. This effect could be alleviated by lowering the desired velocity poles in the cue law at the expense of velocity performance and higher gains on the acceleration and stick terms.

The display did provide adequate information about the location and velocity of the aircraft relative to the desired touchdown point. Of the pilot comments, one stated that "situation information needs to be presented to the pilot in a format that is easy to interpret to confirm the correctness of the programmed elements of the symbology. In general the display is well designed in this respect, but I was quite surprised how much more critical things became as the ground approached and the need for precision increased" (in addition to the 2 ft desired landing requirement, the rotorcraft's high center of gravity required that the lateral velocity at touchdown be kept small to prevent it from overturning). This comment was especially true for the RCAH system, where as long as the aircraft was not in the near proximity to the ground, all of the pilots were willing to maneuver freely and were reasonably able to reach the pad and begin a descent. Yet, as the ground approached on the display, the downwash-induced aircraft motion and, therefore, the position errors increased. The combination of a somewhat poorly augmented control and display combination, aircraft vibration, any display clutter, high pilot gains to minimize small errors, and anxiety due to the ground proximity all led to a stress-induced workload. Achieving this effect of stress-induced workload is seldom possible with ground-based simulation.

Some precision difficulties appear to be related to the impression of display clutter during the final landing phase when many symbols become superimposed at the origin. This clutter makes small cue and velocity errors difficult to see and denies the pilot the essential lead information needed to maintain a precise position. The problem was aggravated by the fact that the desired (less than 2 ft) position errors were difficult to perceive, and with overlaid symbols it was possible to mistake one for the other.

To relieve some display clutter effects, one pilot suggested that the primary symbology elements, such as the acceleration cue and the trident symbol, be made more prominent by increasing their line widths. When the trident is collocated over the pad, the trident noseboom line can be confused with the wind vector line. Occasionally, this caused a pedal input in the wrong direction. If the noseboom were made bolder, by increasing line width, the confusion might be alleviated. This concept of emphasizing symbols that are key to the task clearly has merit as a general display requirement.

Overall, the factor leading to the most advanced configurations (TVC and ACAH with vertical damping) being rated level 2 rather than level 1 resulted from the moderate level of workload involved in zeroing out the station-keeping error in the final stage of the landing to meet the desired 2 ft landing dispersion. This workload resulted from suppressing the external disturbances in a heavily vibratory environment during a demanding and potentially safety critical portion of the task, namely the touchdown.

Conclusions

This paper describes the in-flight evaluation of control and display concepts on a variable-stability helicopter. A new display design procedure was developed that is centered on attaining constant vehicle velocity performance with pilot-loop closure regardless of the level of control augmentation. In addition, the display design is integrated with a task guidance law to achieve acceptable positioning performance. With pilots using a display that simultaneously integrated horizontal and vertical command and status information, one-half of the 28 blind landings were performed to within 2 ft of the desired touchdown point.

Although desired performance was achieved in flight for both the attitude and velocity command systems, the vibratory environment of the CH-47B and the workload associated with the final few seconds before touchdown caused average handling qualities ratings to be level 2 for these command/response types. For the attitude-rate command system, landings were not attempted owing to excessive pilot workload. With this level of control system augmentation, more attention needs to be given to the tradeoff between acceptable pilot workload at the expense of decreased achievable task performance.

Acknowledgments

Many key personnel are responsible for the success of this flight experiment. The authors thank Bill Hindson and Michelle Eshow for their technical ideas; evaluation pilots Jim Martin, Gordon Hardy, and Mike Stortz for their valuable comments; safety pilot George Tucker; crew chief Perry Silva; and assistant crew chief Roy Williams.

References

[1]Kelly, J. R., Niessen, F. R., Thibodeaux, J. J., Yenni, K. R., and Garren, J. F., Jr., "Flight Investigation of Manual and Automatic VTOL Decelerating Instrument Approaches and Landings," NASA TN D-7524, July 1974.

[2]Demko, P. S., and Boschma, J. H., "Advances in Decelerating Step Approach and Landing for Helicopter Instrument Approaches," Paper 79-16, American Helicopter Society 35th Annual National Forum, Washington, DC, May 1979.

[3]Downing, D. R., Bryant, W. H., and Ostroff, A. J., "Flight Test of a VTOL Digital Autoland System Along Complex Trajectories," AIAA Paper 79-1703, Aug. 1979.

[4]Kelly, J. R., and Niessen, F. R., "Navigation, Guidance, and Control for Helicopter Automatic Landings," NASA TP-1649, May 1980.

[5]Merrick, V. K., "Study of the Application of an Implicit Model-Following Flight Controller to Lift-Fan VTOL Aircraft," NASA TP-1040, Nov. 1977.

[6]Merrick, V. K., and Gerdes, R. M., "Design and Piloted Simulation of a VTOL Flight-Control System," *Journal of Guidance and Control,* Vol. 1, No. 3, 1978, pp. 209–216.

[7]Merrick, V. K., "Simulation Study of Two VTOL Control/Display Systems in IMC Approach and Landing," NASA TM-81295, Aug. 1981.

[8]Merrick, V. K., "A Translational Velocity Command System for VTOL Low-Speed Flight," NASA TM-84215, March 1982.

[9]Farris, G. G., Merrick, V. K., and Gerdes, R. M., "Simulation Evaluation of Flight Controls and Display Concepts for VTOL Shipboard Operations," AIAA Paper 83-2173, Aug. 1983.

[10]Merrick, V. K., and Gerdes, R. M., "VTOL Controls for Shipboard Operations," SAE Paper 831428, Society of Automotive Engineers, New York, Oct. 1983.

[11]Merrick, V. K., "Simulation Study of Two VTOL Control/Display Systems in IMC Approach and Shipboard Landing," NASA TM-85996, Dec. 1984.

[12]Lebacqz, J. V., Merrick, V. K., and Franklin, J. A., "Control and Display Requirements for Decelerating Approach and Landing of Fixed- and Rotary-Wing VSTOL Aircraft," Paper A-86-42-70-1000, American Helicopter Society 42nd Annual National Forum, Washington, DC, June 1986.

[13]Moralez, E., Merrick, V. K., and Schroeder, J. A., "Simulation Evaluation of an Advanced Control Concept for a V/STOL Aircraft," *Journal of Guidance, Control, and Dynamics,* Vol. 12, No. 3, 1989, pp. 334–341.

[14]Foster, J. D., Moralez, E., Franklin, J. A., and Schroeder, J. A., "Integrated Control and Display Research for Transition and Vertical Flight on the NASA V/STOL Research Aircraft (VSRA)," SAE Paper 872329, Society of Automotive Engineers, New York, Oct. 1987 (see also NASA TM-100029, Oct. 1987).

[15]Hindson, W. S., Hilbert, K. B., Tucker, G. E., Chen, R. T. N., and Fry, E. B., "New Capabilities and Recent Research Programs of the NASA/Army CH-47B Variable-Stability Helicopter," *Proceedings of the American Helicopter Society 42nd Annual National Forum,* Washington, DC, 1986.

[16]Hindson, W. S., and Tucker, G. E., "Development and Flight Test of a Precision Autohover Capability for Tactical Rotorcraft," American Helicopter Society 44th Annual National Forum, Washington, DC, June 1988.

[17]Hilbert, K. B., Lebacqz, J. V., and Hindson, W. S., "Flight Investigation of a Multivariable Model-Following Control System for Rotorcraft," AIAA Paper 86-9779, April 1986.

[18]Tischler, M. B., "Frequency Response Identification of XV-15 Tilt-Rotor Dynamics," NASA TM-89428, May 1987.

[19]Hodgkinson, J., and Buckley, J., "NAVFIT User's Guide," Naval Air Development Center, Warminster, PA, Oct. 1978.

[20]*Handling Qualities Requirements for Military Rotorcraft,* U.S. Army AVSCOM Aeronautical Design Standard ADS-33C, St. Louis, MO, Aug. 1989.

[21]Hoh, R. H., and Mitchell, D. G., "Proposed Revisions to MIL-F-83300 V/STOL Flying Qualitites Specification," Naval Air Development Center, NADC-82146-60, Warminster, PA, Jan. 1986.

[22]Radford, R. C., Andrisani, D., II, and Beilman, J. L., "An Experimental Investigation of VTOL Flying Qualities Requirements for Shipboard Landings," Naval Air Development Center, NADC-77318-70, Warminster, PA, Aug. 1981.

[23]Corliss, L. D, and Dugan, D. C., "A VTOL Translational Rate Control System Study on a Six-Degrees-of-Freedom Motion Simulator," NASA TM X-62194, Oct. 1972.

[24]McRuer, D., and Schmidt, D. K., "Pilot-Vehicle Analysis of Multiaxis Tasks," *Journal of Guidance, Control, and Dynamics,* Vol. 13, No. 2, 1990, pp. 348–355.

[25]Merrick, V. K., Farris, G. G., and Vanags, A. A., "A Head Up Display Format for Application to V/STOL Approach and Landing," NASA TM-102216, Jan 1990.

[26]"V/STOL Displays for Approach and Landing," AGARD Rept. 594, July 1972.

[27]Dukes, T. A., Keane, W. P., and Tsoubanos, C. M., "Image and Superimposed Symbology—An Integrated Display for Helicopters," Paper 724, American Helicopter Society 29th Annual National Forum, Washington, DC, May 1973.

[28]Lemons, J. L., "A Study of the Effect of Displayed Acceleration Information on VTOL Hover Performance," M.S.E. Thesis, Princeton Univ., Princeton Rept. 1183-T, Princeton, NJ, Sept. 1974.

[29]Tsoubanos, C. M., and Kelley, M. B., "Pilot Night Vision System (PNVS) for Advanced Attack Helicopter (AAH)," Paper 78-16, American Helicopter Society 34th Annual National Forum, Washington, DC, May 1978.

[30]McRuer, D. T., and Krendel, E. S., "Mathematical Models of Human Pilot Behavior," AGARDograph 188, Jan. 1974.

[31]Weir, D. H., Klein, R. H., and McRuer, D. T., "Principles for the Design of Advanced Flight Director Systems Based on the Theory of Manual Control Displays," NASA CR-1748.

[32]Hynes, C. S., Franklin, J. A., Hardy, G. H., Martin, J. L., and Innis, R. C., "Flight Evaulation of Pursuit Displays for Precision Approach of Powered-Lift Aircraft," *Journal of Guidance, Control, and Dynamics,* Vol. 12, No. 4, 1989, pp. 521–529.

[33]Eshow, M. M., "Flight Investigation of Variations in Rotorcraft Control and Display Dynamics for Hover," AIAA Paper 90-3482, Aug. 1990.

[34]Hess, R. A., and Gorder, P. J., "Design and Evaluation of a Cockpit Display for Hovering Flight," *Journal of Guidance, Control, and Dynamics,* Vol. 13, No. 3, 1990, pp. 450–457.

[35]Garg, S., and Schmidt, D. K., "Cooperative Synthesis of Control and Display Augmentation," AIAA Paper 86-2204, Aug. 1986.

[36]Cooper, G. E., and Harper, R. P., Jr., "The Use of Pilot Rating in the Evaluation of Aircraft Handling Qualities," NASA TN D-5153, April 1969.